Journal of Geophysical Research: Solid Earth

Supporting Information for

Major Disruption of D″ beneath Alaska

Daoyuan Sun[1,2], Don Helmberger[3], Meghan S. Miller[4], and Jennifer M. Jackson[3]

[1]Laboratory of Seismology and Physics of Earth's Interior, School of Earth and Space Sciences, University of Science and Technology of China, Hefei, Anhui 230026, China;
[2]National Geophysics Observatory at Mengcheng, Anhui 233500, China;
[3]Seismological Laboratory, California Institute of Technology, Caltech, Pasadena, CA 91125;
[4]Department of Earth Sciences, University of Southern California, Los Angeles, CA 90089.

Contents of this file

Introduction

The supporting figures provide a series of synthetics tests on the detailed D″ structure, complete S data for event 20111021 (Fig. S3), stacked records of shallow events (Tab. S1 and Fig. S13), the differential travel times between ScS and S (Fig. S7), data and synthetics of sS for the event 20130524 (Fig. S12), and P data for event 20131001 (Fig. S10).

Reference

Matzel, E., M. K. Sen, and S. P. Grand (1996), Evidence for anisotropy in the deep mantle beneath Alaska, *Geophys. Res. Lett*., 23(18), 2417-2420, doi:10.1029/96GL02186.

Sun, D., and D. Helmberger (2008), Lower mantle tomography and phase change mapping, *J. Geophys. Res*., 113 (B10), B10305, doi:10.1029/2007JB005289.

Sun, D., and D. Helmberger (2011), Upper-mantle structures beneath USArray derived from waveform complexity, *Geophys. J. Int*., 184 (1), 416-438.

Young, C. J., and T. Lay (1990), Multiple phase analysis of the shear velocity structure in the D″ region beneath Alaska, *J. Geophys. Res.*, *95*(B11), 17385-17402, doi:10.1029/JB095iB11p17385.

Table S1. Lists of part of the Earthquakes studied

Event date	Lat. (°)	Lon. (°)	Depth (km)	Mw	Remark
20091210	53.42	152.76	656.2	6.3	Distance is less than 75°
20091224	42.23	134.70	410.9	6.3	Distance is less than 75°
20100218	42.59	130.70	577.7	6.9	Used in modeling
20100725	49.70	154.64	130.0	5.6	Not so many data around 75-80°
20101130	28.36	139.15	486.7	6.8	Source is complicate
20111021	43.89	142.48	187.0	6.1	Used in modeling
20111209	47.01	144.55	392.2	5.8	Event is too small to see strong S arrivals
20120814	49.80	145.06	583.2	7.7	Event is too big
20130405	42.74	131.00	563.3	6.4	Distance is larger than 80°
20130524	52.24	151.44	624.0	6.7	Similar as event 20131001
20131001	53.20	152.81	586	6.7	Used in modeling
20100704	39.70	142.37	27.0	6.3	Shallow
20110315	40.33	143.29	19.8	6.1	
20110622	39.96	142.21	33.0	6.7	
20110804	48.83	154.77	36.0	6.1	
20120523	41.33	142.08	46.0	6.0	
20120708	45.50	151.29	20.0	6.0	
20121116	49.28	155.43	29.0	6.5	Events

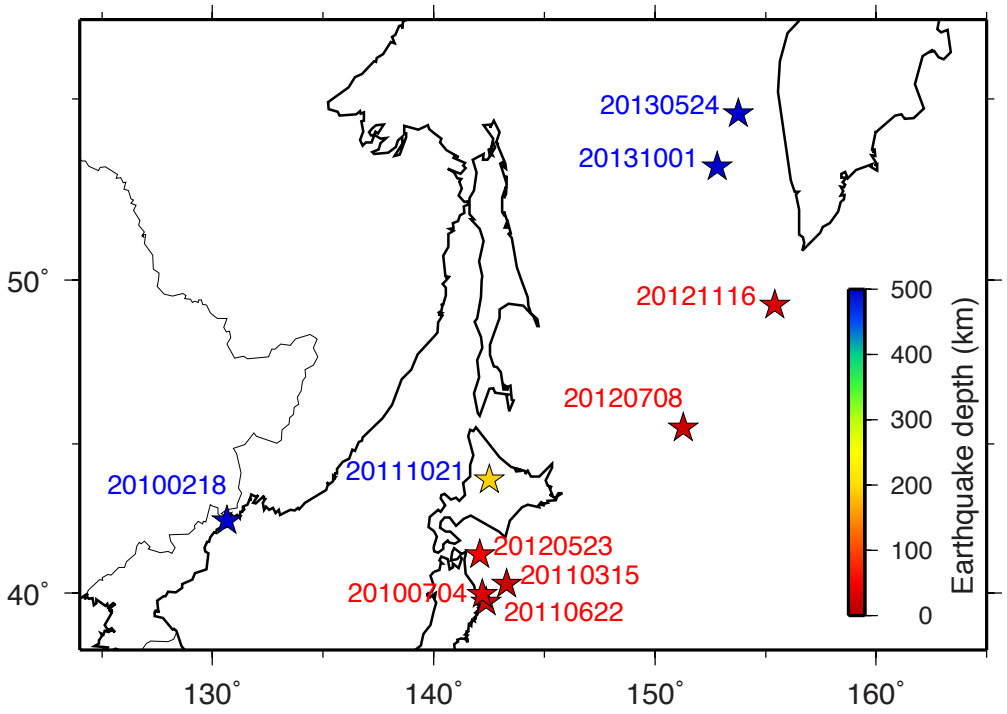

Figure S1. Location of the events used in this study. Shallow events are dispalyed in red stars. The four deep events modeled are displayed in blue and yellow stars.

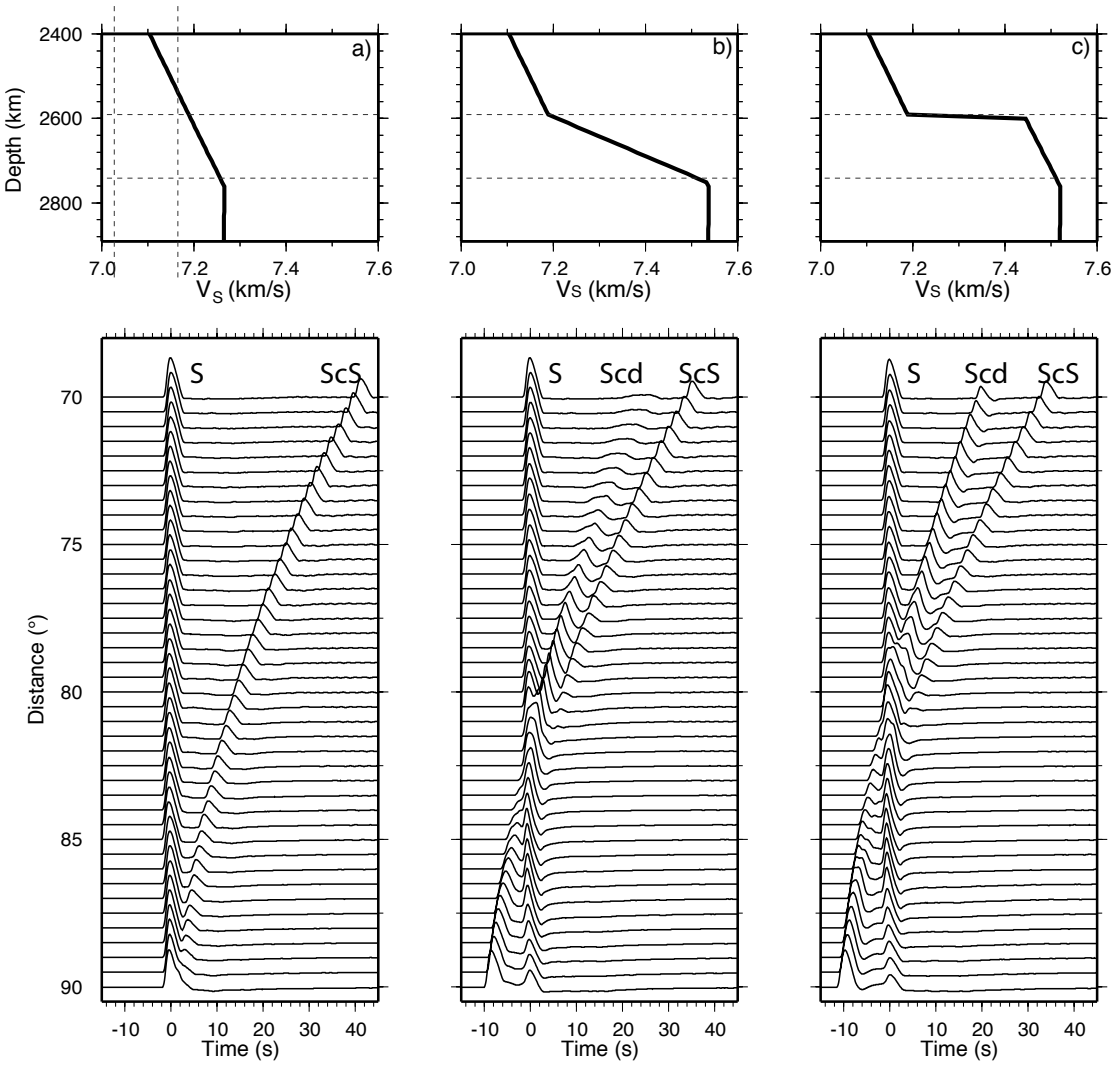

Figure S2. The synthetics for possible 1-D models of D". (a) The PREM model and the synthetics do not have the Scd phase. (b) A linear velocity gradient and produces the extra Scd phase between S and ScS. (c) A sharp velocity jump plus a gradient velocity jumps in the model, simulating a complex transition zone (After *Sun and Helmberger*, 2008).

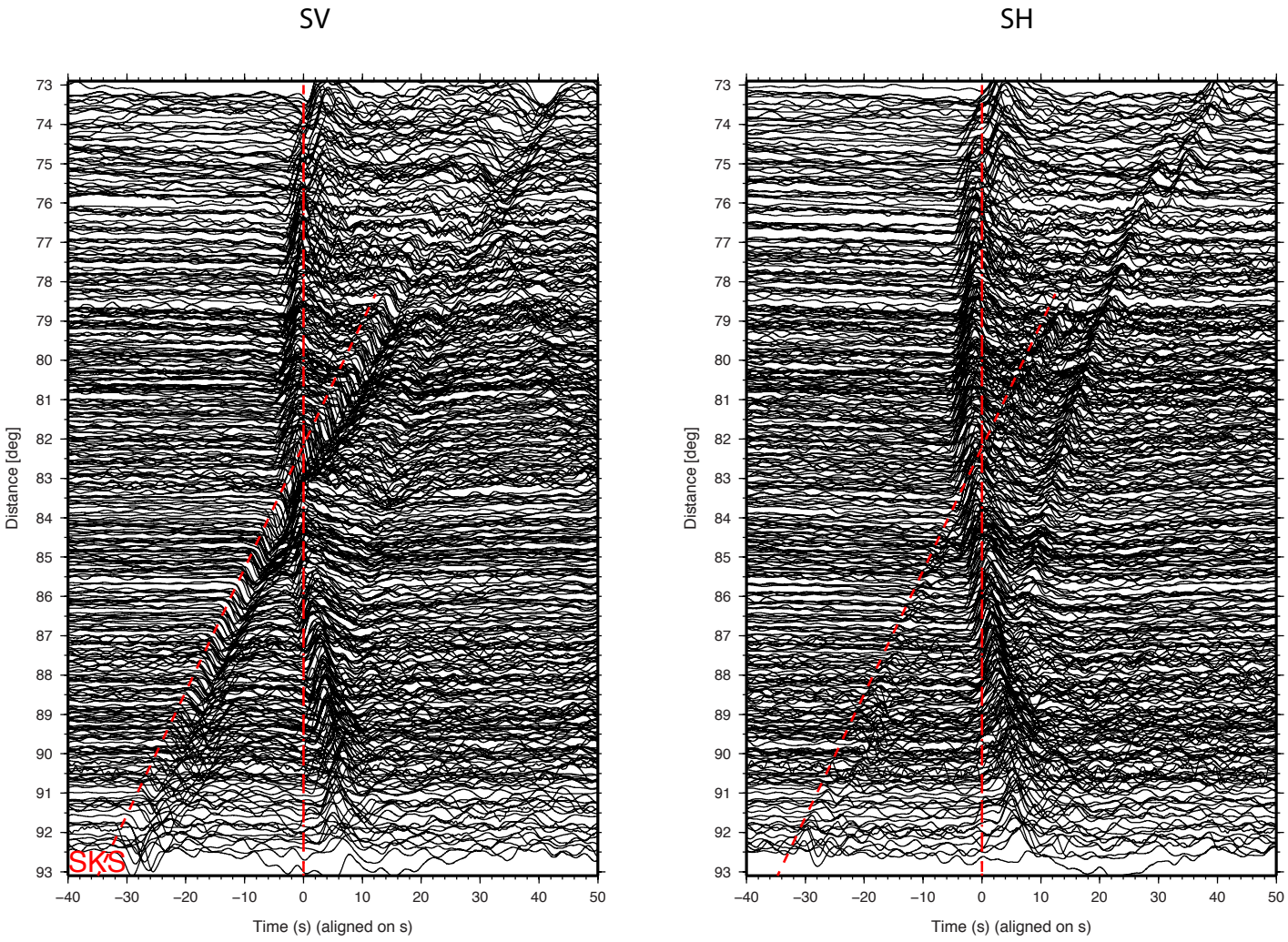

Figure S3. Data record sections for event 20111021. Note there are no obvious Scd arrivals for distance less than 80° on both the SH and SV sections. The red oblique dash lines indicates the SKS arrivals, which are also seen on SH components making it difficult to identify Scd.

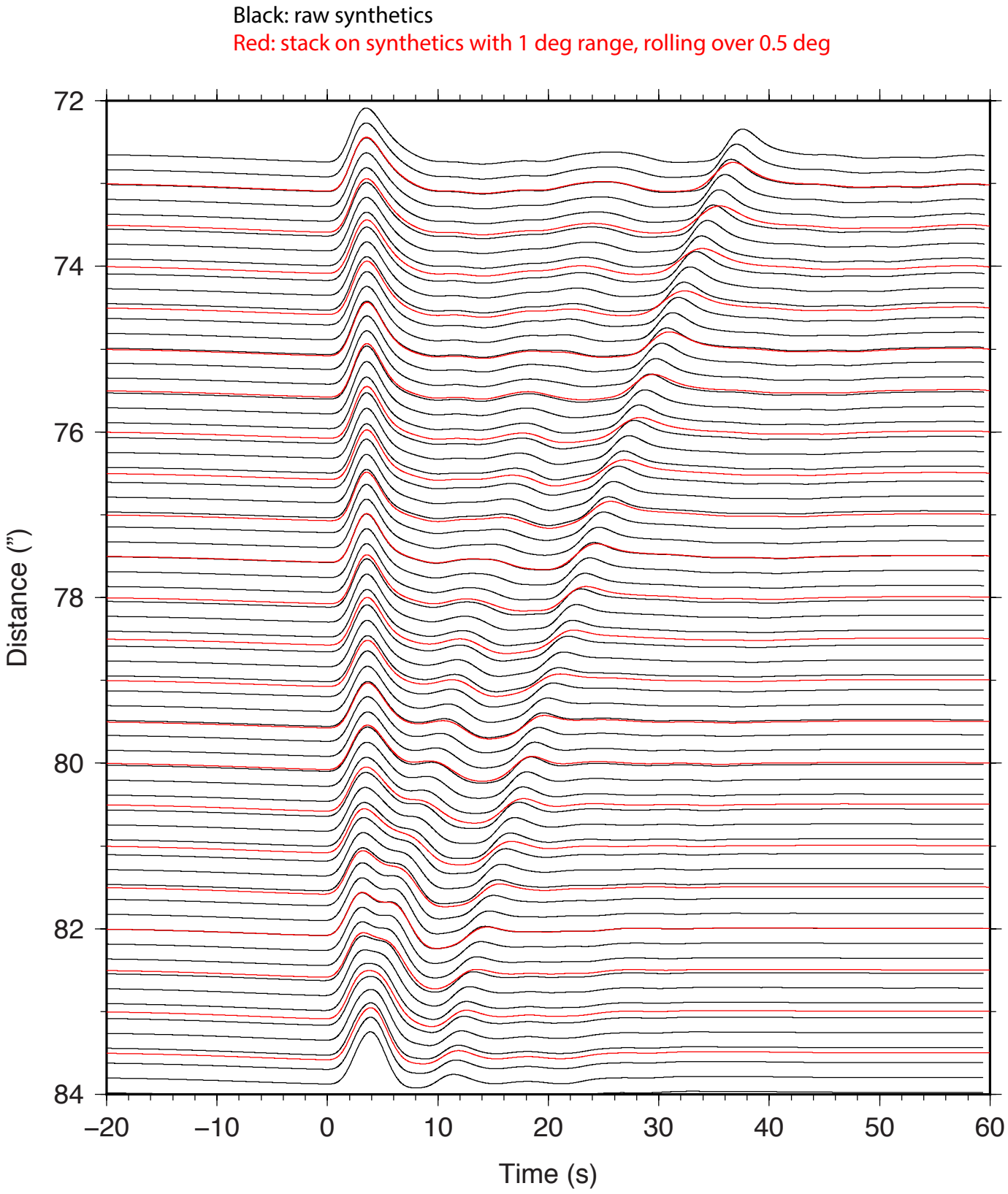

Figure S4. Examples of stacking the synthetics. Red traces are the stacking over 0.5° for the generated synthetics (black). Such stacking does broaden the ScS waveforms.

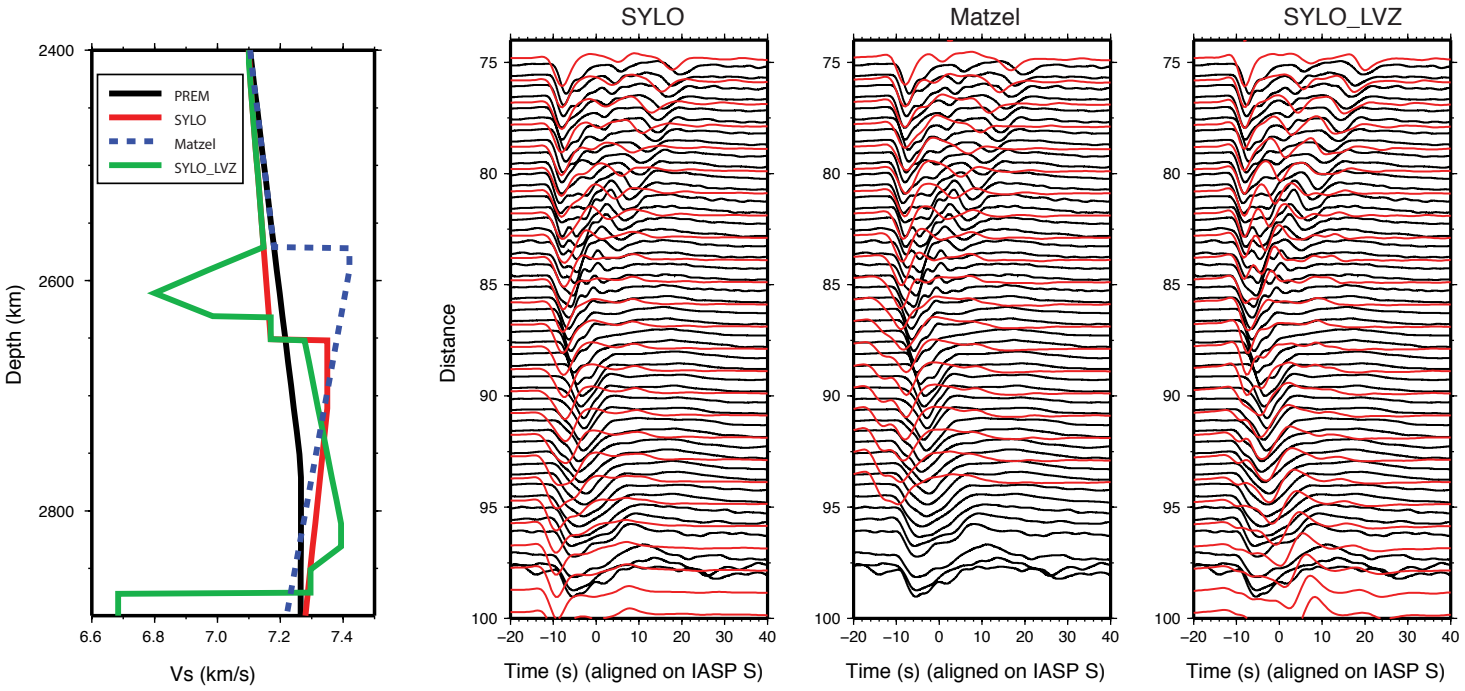

Figure S5. 1D models and (B) related synthetics (red traces) together with data (black traces, western event). SYLO [*Young and Lay*, 1990] describe the S and Scd behavior very well up to 82°. The model Matzel is from *Matzel et al.* [1996]. The earlier ScS arrivals and the S at larger distance suggest a slower layer beneath. The SYLO_LVZ model has the ability to describe the abrupt delay at ~90°, but disrupts the Scd behavior. The structure presented in (A) fits this data at long periods but not in detail. Unfortunately, this data samples the souhtern Rock Mountain Front, especially at large distances where the upper-mantle structure is complex [*Sun and Helmberger*, 2011]. Thus, only the well behaved waveforms at distance less than 85° was used to define the phase transition.

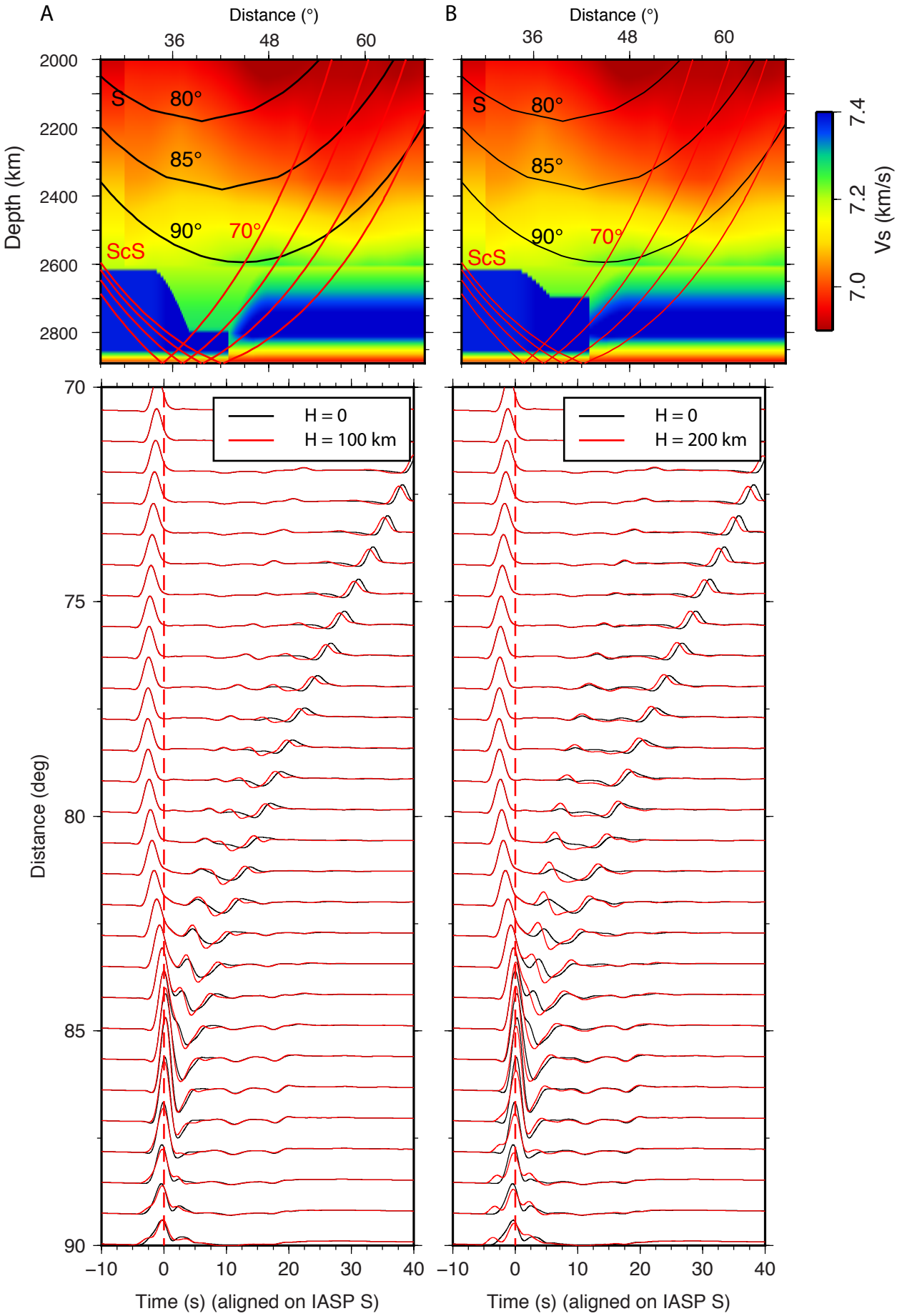

Figure S6. Sensitivity test for the thickness of the D" gap structure discussed in Fig. 6. The model in Fig. 6 has H of 0. When the thickness is 200 km (B), the Scd arrivals become strong near 80°.

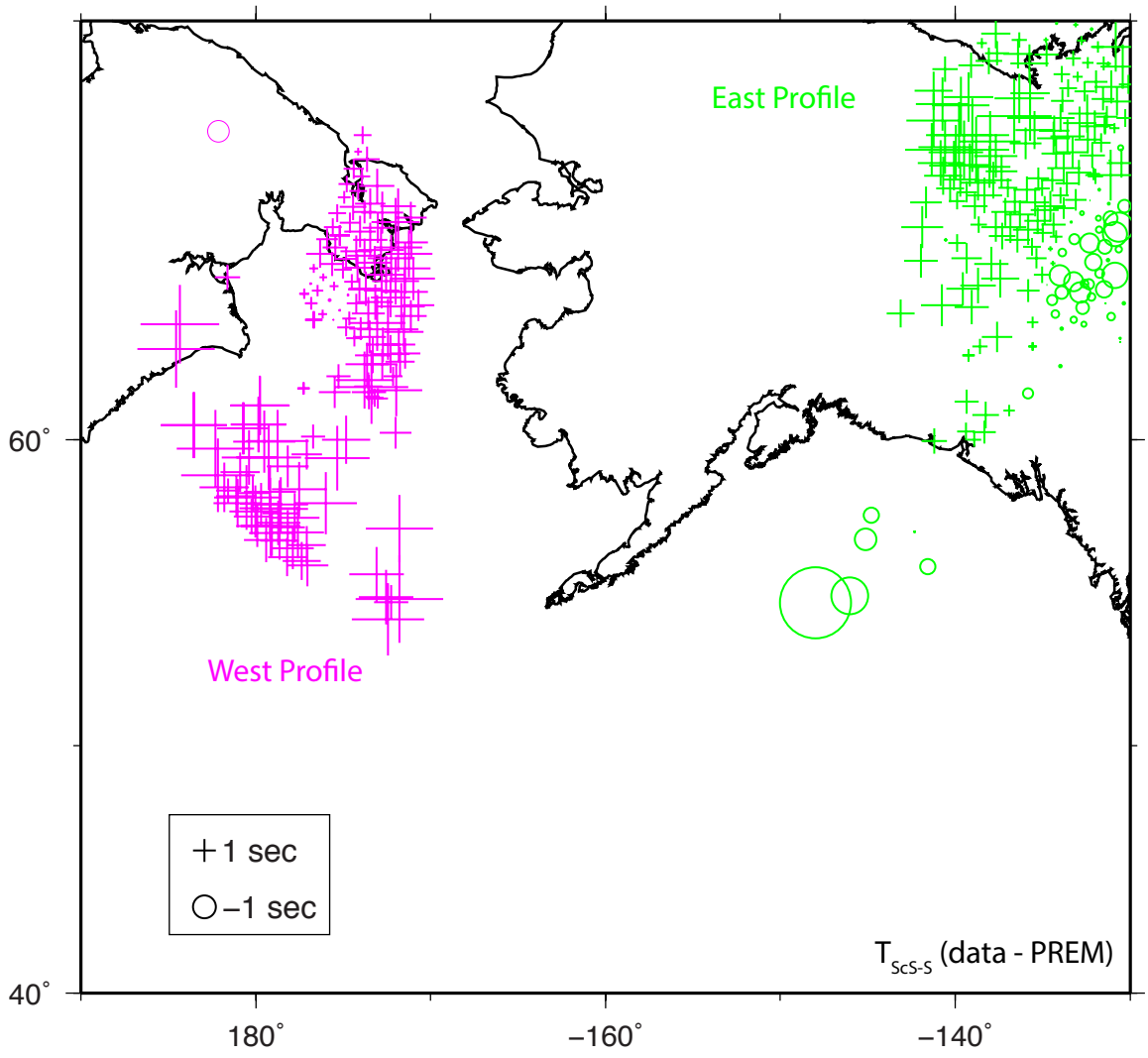

Figure S7. The differential travel time between ScS and S, T_{ScS-S}(data-PREM), for the West Profile (magenta color) and East Profile (green color) events in Fig. 4A. The T_{ScS-S} (data-PREM) values are mapped to the S turning points at the base of mantle.

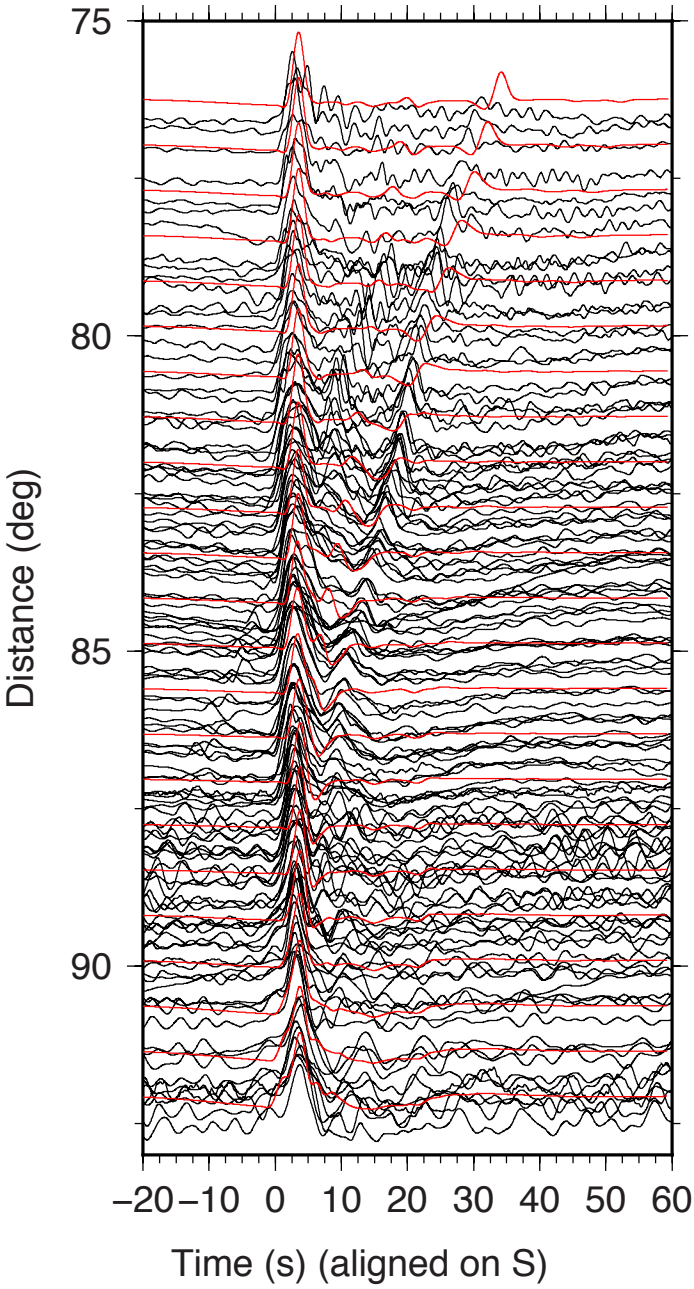

Figure S8. SH synthetics (red) for the plume model as in Fig. 8 and the data (black). The data are only plotted with azimuths between 40° and 44°, which has the anomalous S data (Fig. 7).

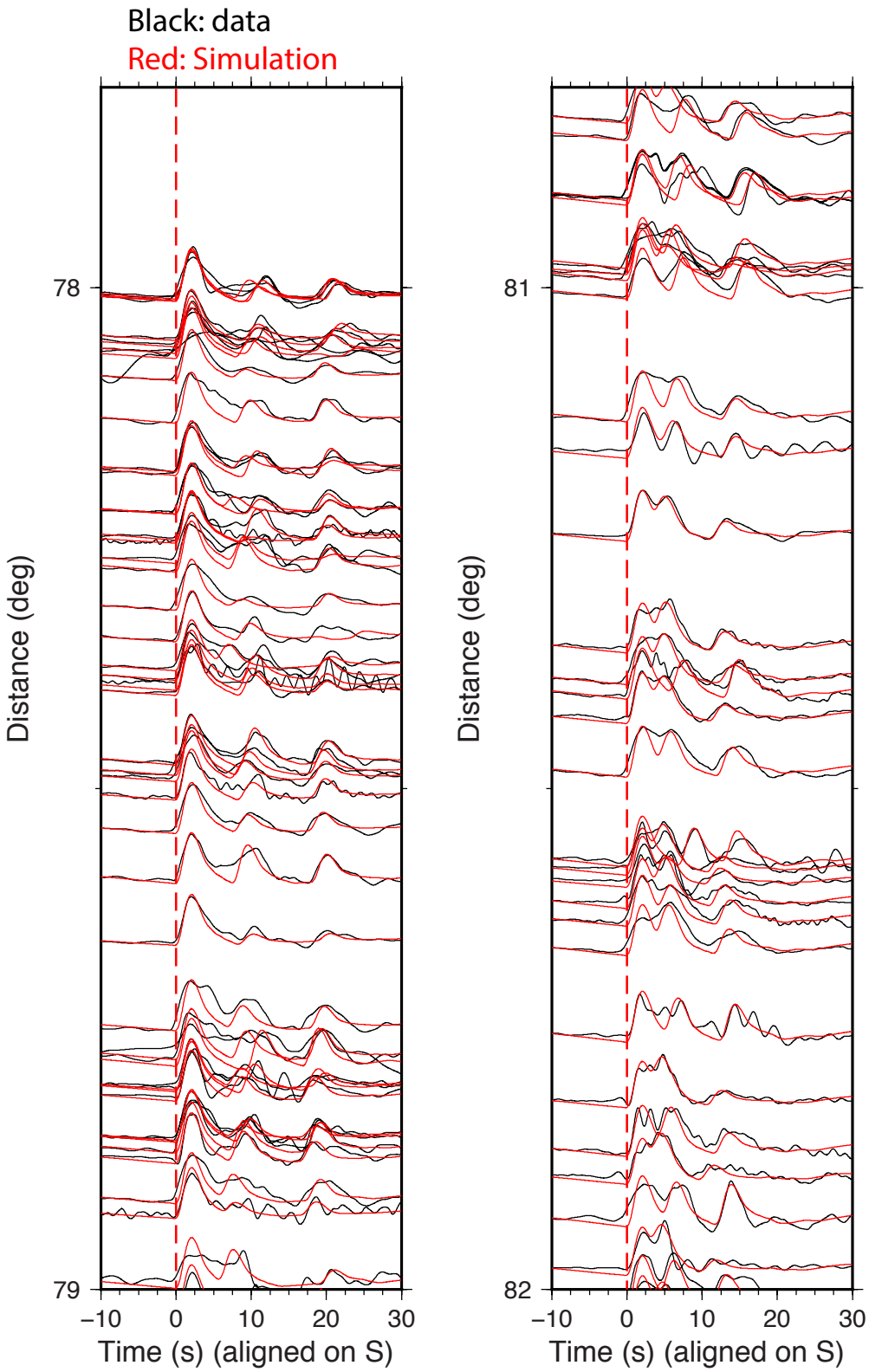

Figure S9. Examples of data (black) and simulations (red) by applying the method displayed in Fig. 11A.

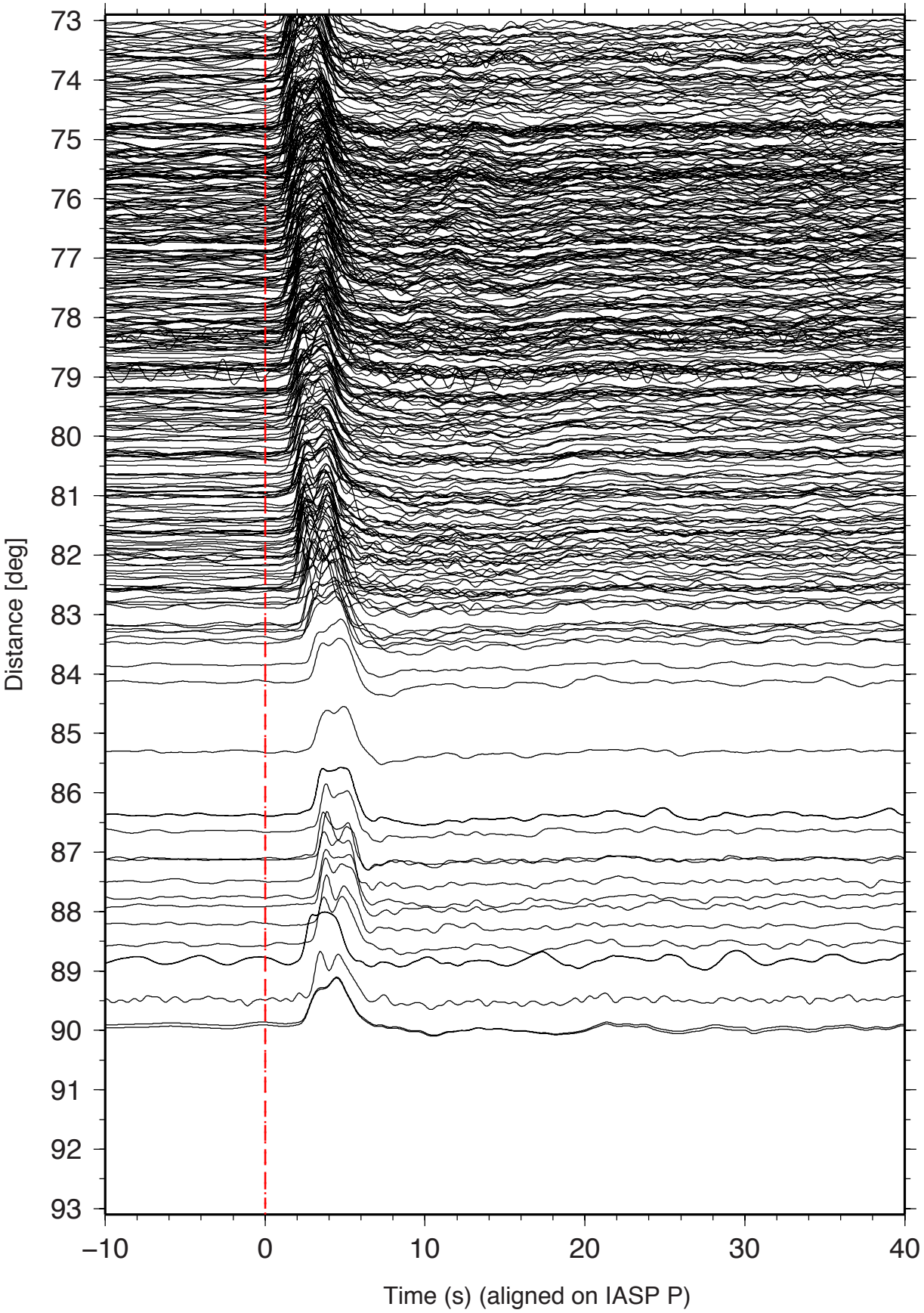

Figure S10. P data for the event 20131001. Note there is no obvious Pcd arrivals present.

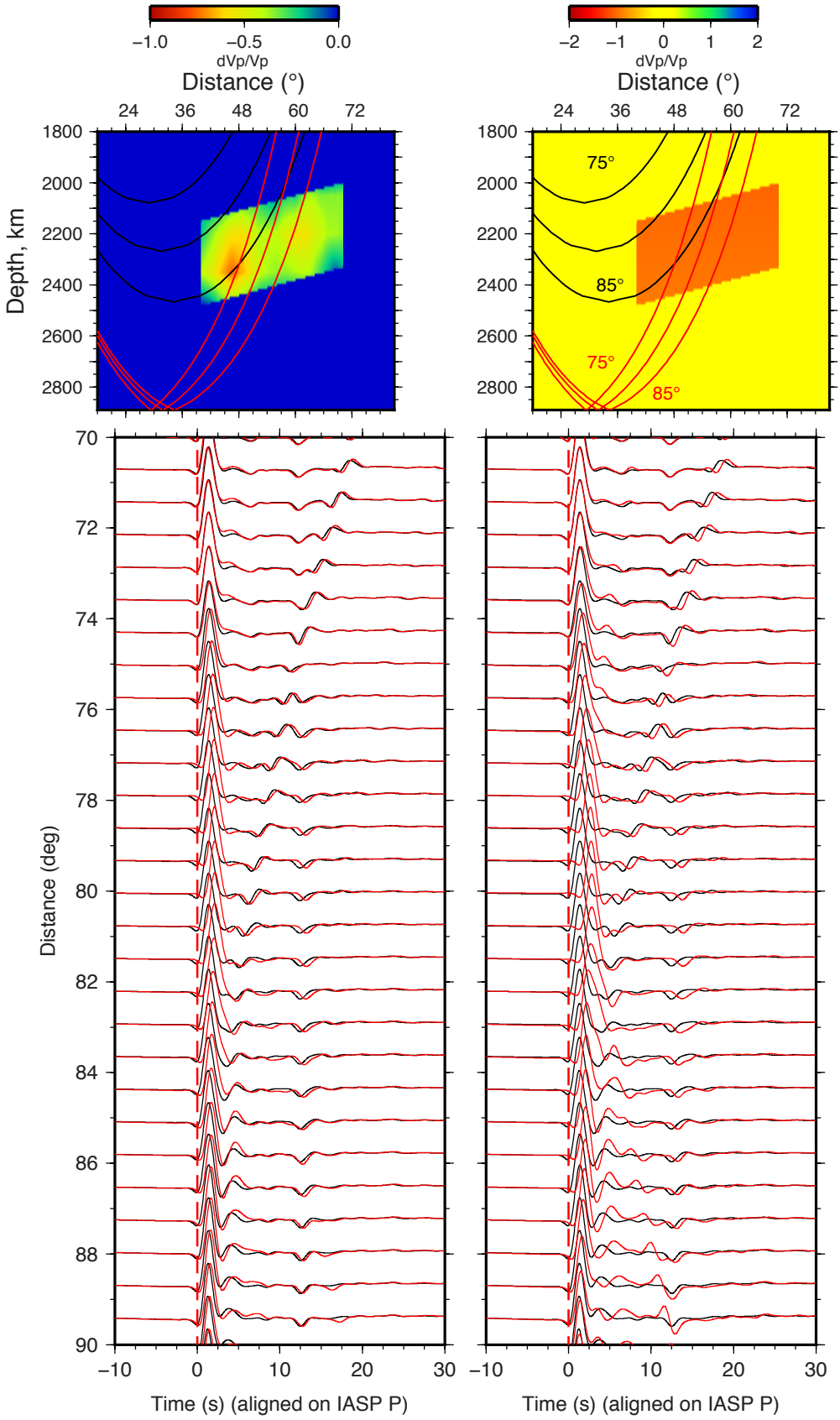

Figure S11. Predictions of the P for the eastern Profile. The black traces are for the model without LVZ above the D". The red traces are the predictions for the LVZ models. The models are set up by highlighting the LVZ above the D" in the orginal GyPSum model. The left model is generateded from the tomograph model by asumming $\delta Vs/\delta Vp=2$. The right model has uniform $\delta Vp=-1.5\%$ in the box.

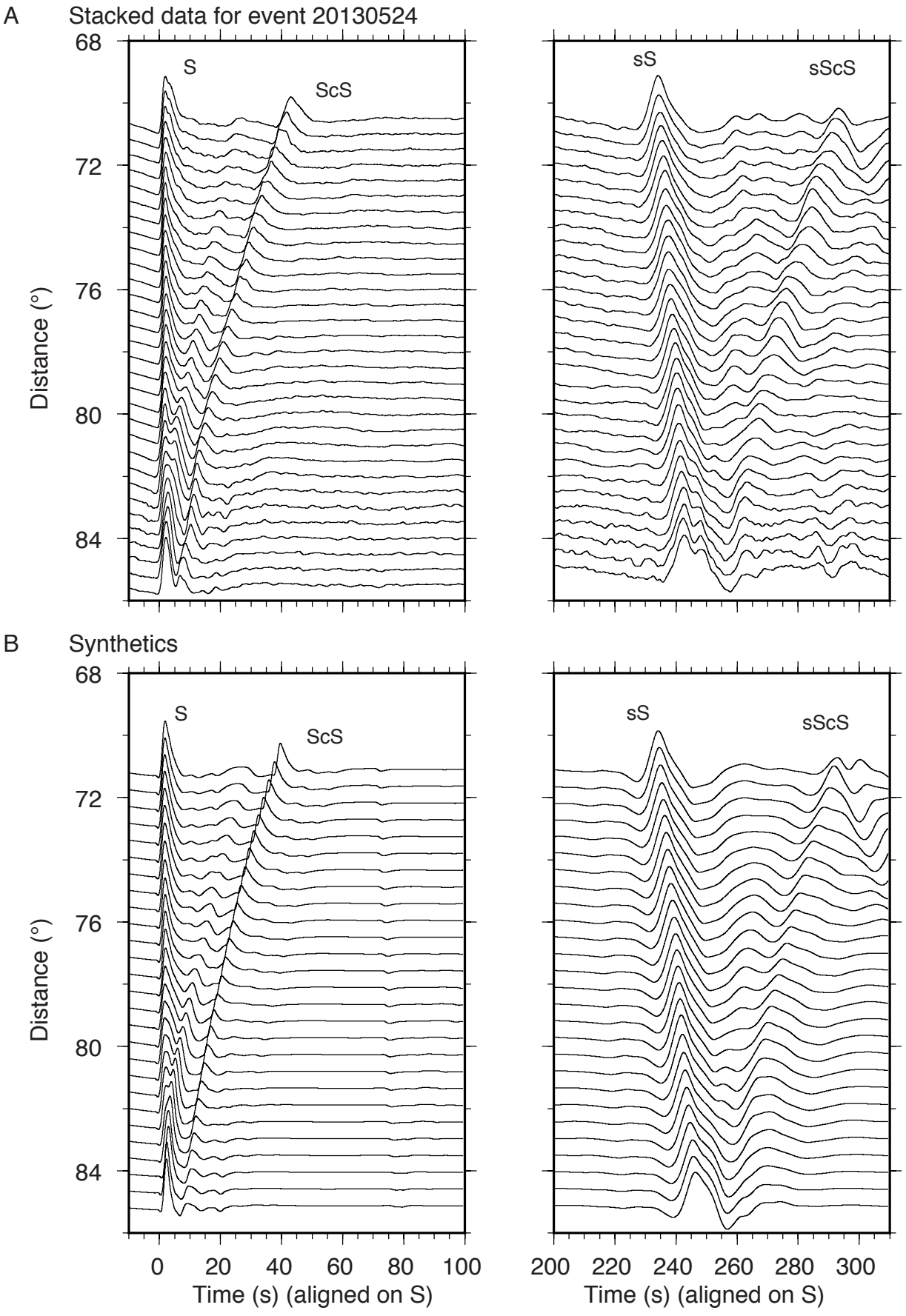

Figure S12. Comparison between S (left column) and sS (right column) for the event 20130524. The stack data are displayed in (A). The synthetics in (B) are generated from the model in Fig. 5A.

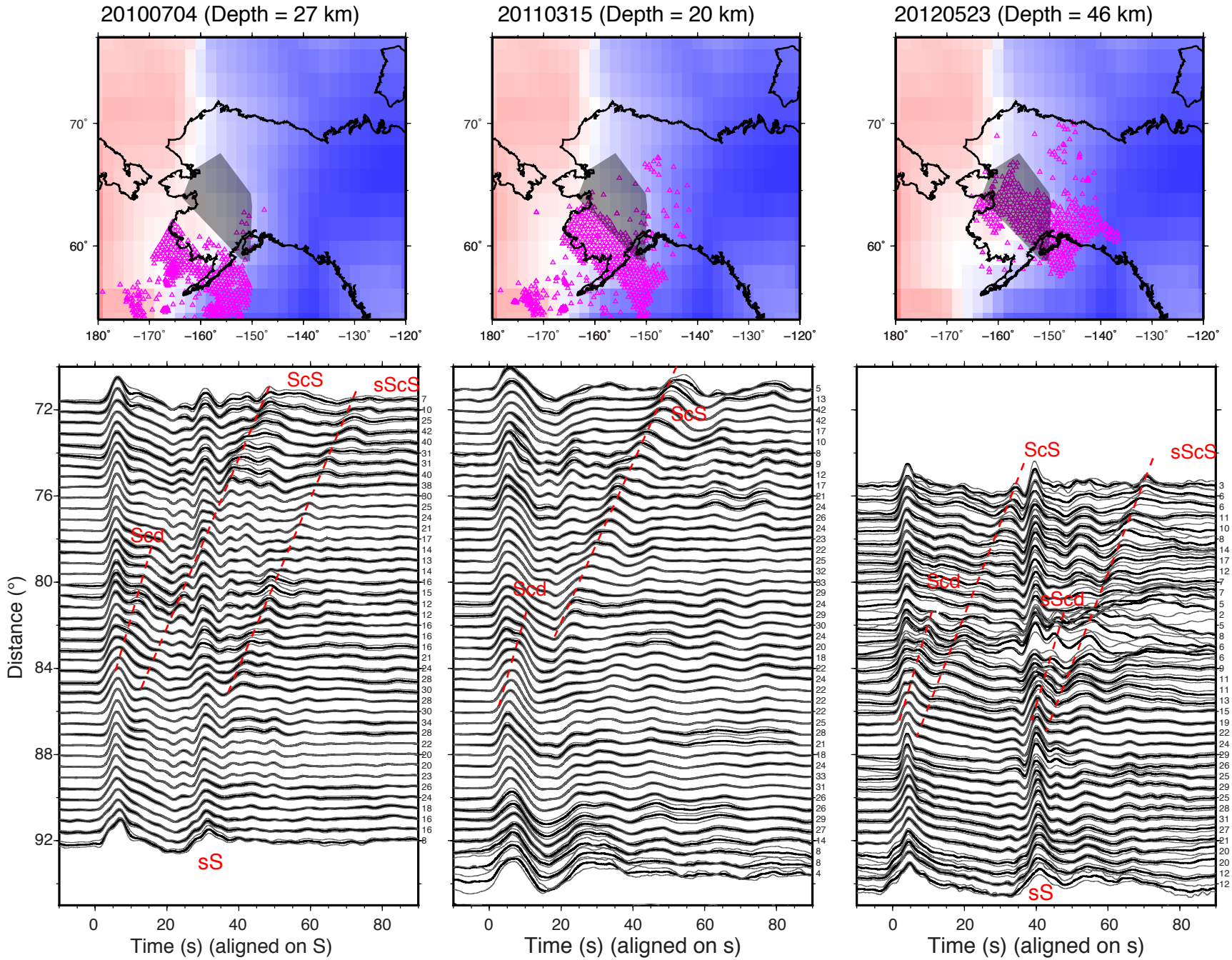

Figure S13. *S*tacked SH records for the shallow events listed in Table S1 and Fig. S1. The top panels are the S turning points together with the GyPSuM model at the base of the mantle. The bottom panels display the stacked SH records. Note that the depth phases interfere with Scd arrivals, which make identifying Scd arrivals difficultly. The numbers after each trace are the number of records included in the stacking process. The gray shaded areas in the top panel display the sampling region of the deep event 20111021 as in Fig. 4.

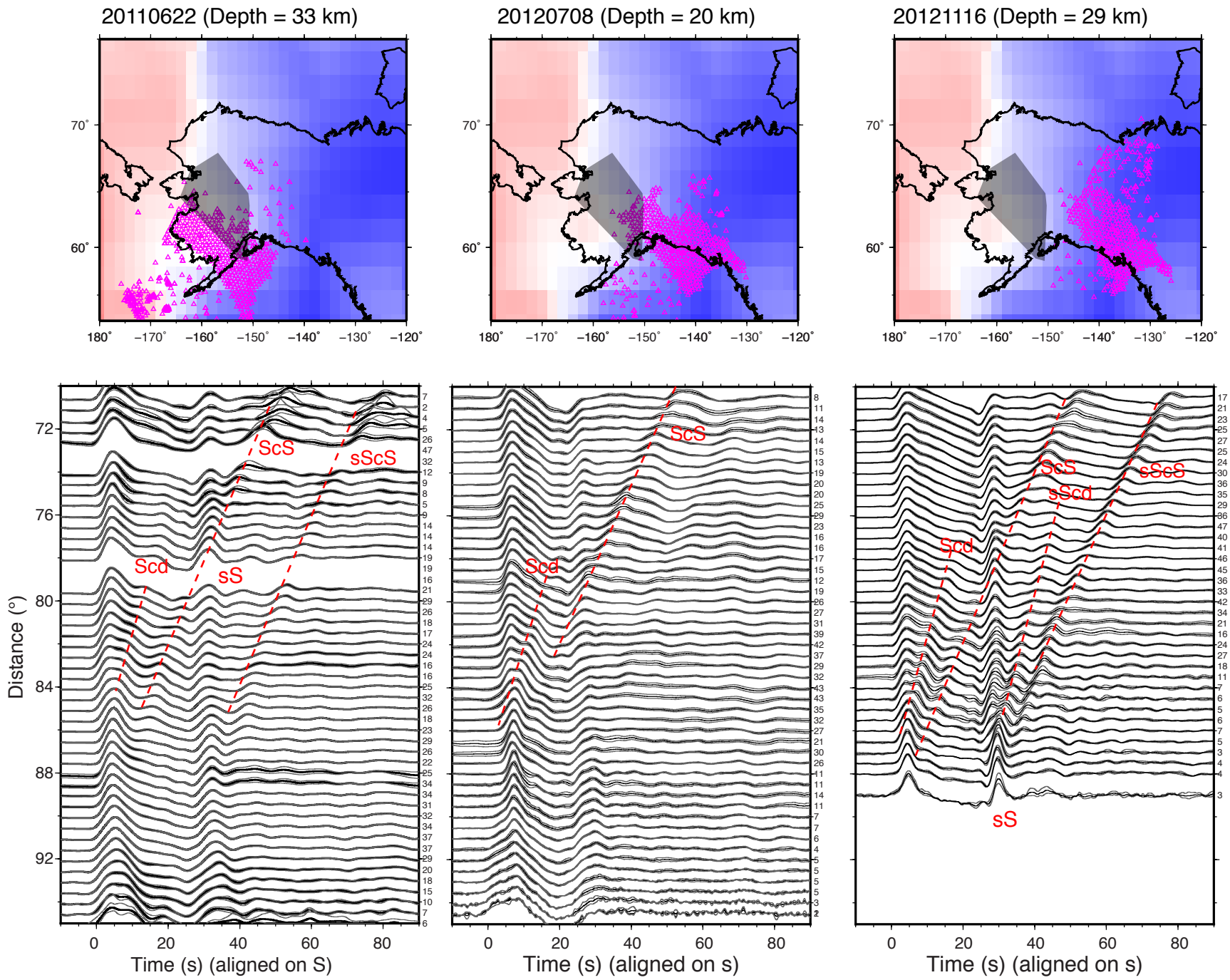

Figure S13 (continued)

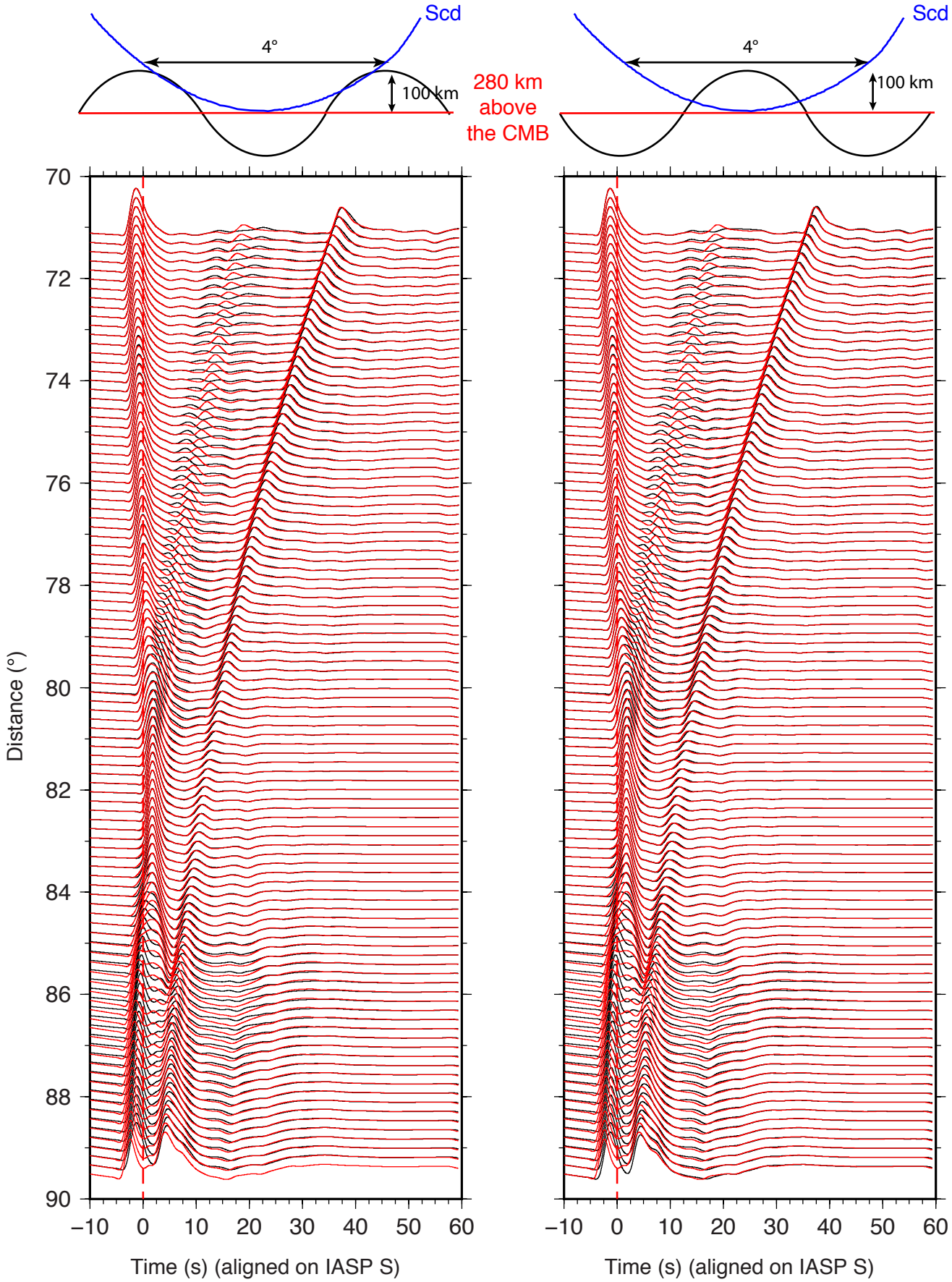

Figure S14. Synthetics for a model with rough D" discontinuity. In the rough model, the top of the D" discontinuity has a sinusoid shape with 100 km variation of the height within a period of 4° across. The black traces are the synthetics for the rough model and the red traces are for the D" model with flat top. The left column has the 80° Scd ray bottoming at the valley of the sinusoid shape and the right column has the ray bottoming at the peak.

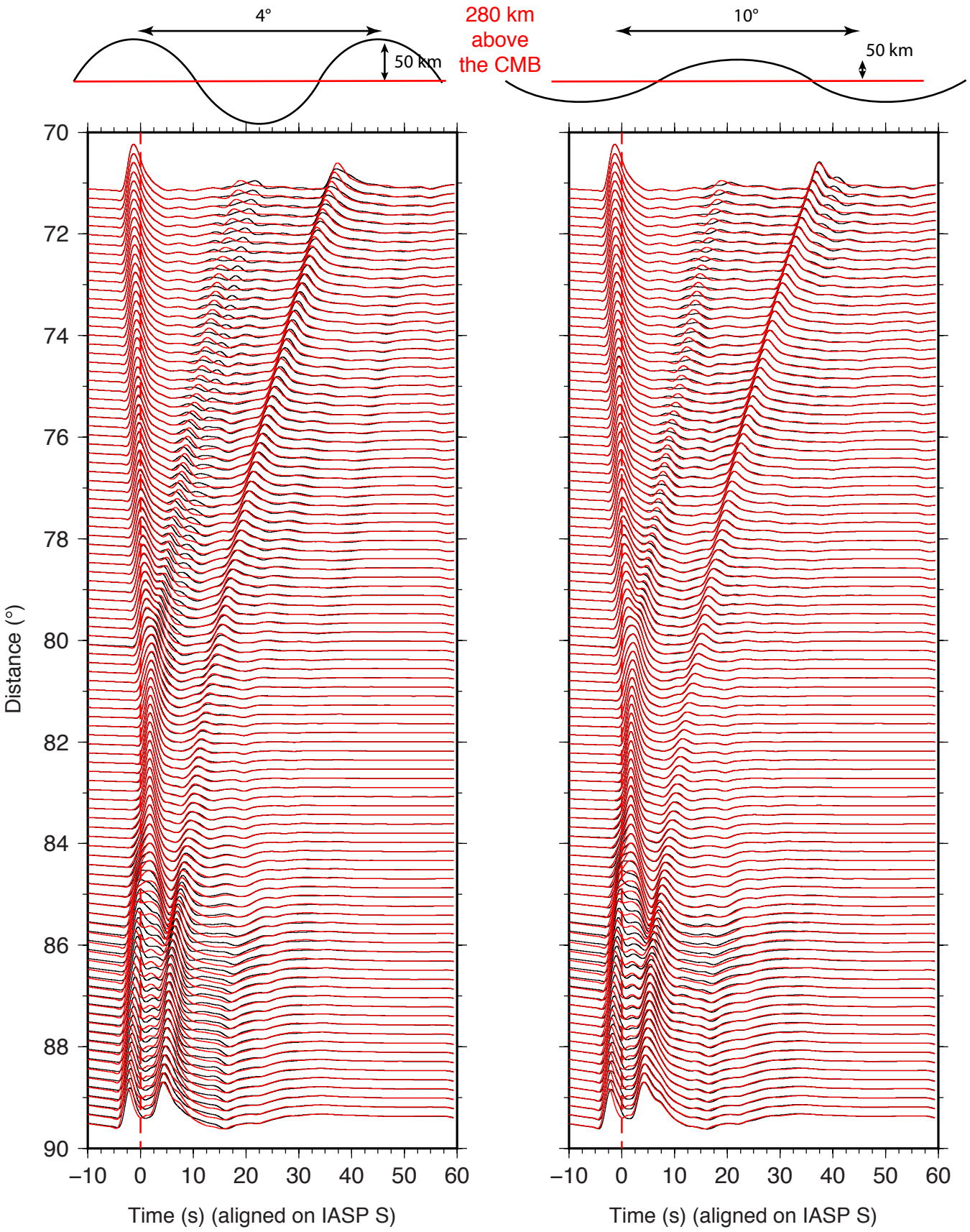

Figure S15. Similar setup to the Fig. S15 but with smaller variation of the height. In the left column, the top of the D" discontinuity has a sinusoid shape with 50 km variation of the height within a period of 4° across. The right column has the shape with 50 km variation of the height within a period of 10°.